



HAL
open science

Divergent Synthesis of Molecular Winch Prototypes

Yohan Gisbert, Seifallah Abid, Claire Kammerer, Gwénaél Rapenne

► **To cite this version:**

Yohan Gisbert, Seifallah Abid, Claire Kammerer, Gwénaél Rapenne. Divergent Synthesis of Molecular Winch Prototypes. *Chemistry - A European Journal*, 2021, 27 (65), pp.16242-16249. 10.1002/chem.202103126 . hal-03636845

HAL Id: hal-03636845

<https://hal.science/hal-03636845>

Submitted on 1 Jun 2022

HAL is a multi-disciplinary open access archive for the deposit and dissemination of scientific research documents, whether they are published or not. The documents may come from teaching and research institutions in France or abroad, or from public or private research centers.

L'archive ouverte pluridisciplinaire **HAL**, est destinée au dépôt et à la diffusion de documents scientifiques de niveau recherche, publiés ou non, émanant des établissements d'enseignement et de recherche français ou étrangers, des laboratoires publics ou privés.

Divergent Synthesis of Molecular Winch Prototypes

Yohan Gisbert,^[a] Seifallah Abid,^[a] Claire Kammerer,^{*[a]} and Gwénaél Rapenne^{*[a,b]}

[a] Y. Gisbert, Dr. S. Abid, Dr. C. Kammerer, Prof. Dr. G. Rapenne
CEMES, Université de Toulouse, CNRS
29, rue Marvig, 31055 Toulouse, France
E-mail: rapenne@cemes.fr

[b] Prof. Dr. G. Rapenne
Division of Materials Science, Nara Institute of Science and Technology
8916-5 Takayama, Ikoma, Nara, Japan

In memoriam Prof. François Diederich (1952-2020), an outstanding mentor, a close friend and a wonderful human being.

Abstract

We report the synthesis of conceptually new prototypes of molecular winches with the ultimate aim to investigate the work performed by a single ruthenium-based molecular motor anchored on a surface by probing its ability to pull a load upon electrically-driven directional rotation. According to a technomimetic design, the motor was embedded in a winch structure, with a long flexible polyethylene glycol chain terminated by an azide hook to connect a variety of molecular loads. The structure of the motor was first derivatized by means of two sequential cross-coupling reactions involving a penta(4-halogenophenyl)cyclopentadienyl hydrotris(indazolyl)borate ruthenium(II) precursor and the resulting benzylamine derivative was next exploited as key intermediate in the divergent synthesis of a family of nanowinch prototypes. A one-pot method involving sequential peptide coupling and Cu-catalyzed azide-alkyne cycloaddition was developed to yield four loaded nanowinches, with load fragments encompassing triptycene, fullerene and porphyrin moieties.

Preprint

Submitted to *Chemistry a European Journal*

INTRODUCTION

The last two decades have witnessed a tremendous increase in the number and type of artificial molecular machines,^[1] with the ultimate recognition by the scientific community being the awarding of the 2016 Nobel Prize in chemistry to the pioneers in the field: J.-P. Sauvage, Sir J.F. Stoddart and B.L. Feringa.^[2] Many among these machines can be considered as technomimetic^[3] analogues of macroscopic daily life objects such as scissors,^[4] wheelbarrows,^[5] syringes,^[6] elevators,^[7] vehicles,^[8] gears^[9] or robotic arms,^[10] among others. Integration of several such machines into multimolecular functional devices would allow the emergence of nanoscale machineries, able to perform complex tasks when fueled with appropriate energy sources. In this regard, molecular motors are key elements among the wide variety of machines, as they convert chemical, light and electric energy into mechanical energy.^[11] A few groups, including us, have designed, synthesized and studied rotary molecular motors in solution, on nanoparticles,^[12] in liquid crystals,^[13] in gels^[14] or on surfaces^[11d-g] to prove that their actuation could lead to directional motion. Once this milestone achieved, it became highly desirable to access the amount of work performed by molecular motors (e.g. through direct investigations by Single Molecule Force Spectroscopy or magnetic tweezers)^[15] and determine whether such motors can be used for mechanical applications. For example, Feringa et al. doped a liquid crystal with a rotary molecular motor which, stimulated by light, induced a modification of the structure of the liquid crystal, leading to the motion of a glass rod several thousand times larger than these engines.^[13] An example of the use of such motors to induce macroscopic movements has been reported by Giuseppone et al. They formed a gel consisting of motors whose rotors and stators are connected by polyethylene glycol (PEG) chains.^[14] Upon photoirradiation, the motors start to rotate which causes the PEG chains to wind up and as a consequence the motors to come together, finally leading to a macroscopic contraction of the gel. These pioneering studies demonstrated that molecular motors are capable of producing work, which may be recovered up to the macroscopic scale when collective behaviors are implemented.

In this context, our aim is to investigate at the single-molecule scale the mechanical properties of the ruthenium-based molecular motor we developed, which was specifically designed for on-surface studies by Scanning Tunneling Microscopy at Low Temperature (LT-STM) (Figure 1a).^[11e] The architecture of this molecular motor is based on a piano-stool ruthenium(II) complex, with rigid pentaaryl cyclopentadienyl and hydrotris(indazolyl) borate ligands acting as rotor (in blue) and stator (in black), respectively.^[16] The scorpionate tripod is functionalized with three terminal thioether groups to ensure tight adsorption on metal surfaces, thus preventing rotation, translation and rocking motion of the whole complex during STM studies.^[17] In addition, this subunit is designed to lift up the ruthenium ball bearing and thus the cyclopentadienyl platform, whose azimuthal rotation becomes favored over other degrees of freedom. On a Au(111) surface under Ultra-High Vacuum at 5 K, this ruthenium complex is initially motionless and it has been shown that a voltage pulse applied via the STM tip on one of the cyclopentadienyl substituents triggers unidirectional motion of the rotor subunit. Moreover, the direction of rotation is controlled by the location of the tip over the desymmetrized rotor during the inelastic electron tunneling process, with an excitation of the shorter tolyl group or of one of the ferrocenylphenyl fragments resulting in opposite motions. This organometallic structure thus behaves as a motor, able to convert electric energy into directed motion, and it was next envisioned to probe the capacity for this surface-bound motor to perform work, i.e. to move a load on a surface.

To this aim, the ruthenium-based motor was embedded in a molecular winch structure (Figure 1b), including a long flexible chain (in green) and a terminal hook connected to a molecular load (in orange). In this concept, the nanowinch will be deposited onto a metallic surface at low temperature and the molecular load will be pushed away from the motor subunit by lateral manipulation using the STM tip. Subsequent excitation of the motor via a voltage pulse applied with the STM tip is expected to induce a

unidirectional rotation of the pentaarylcyclopentadienyl fragment, and the resulting motion of the load will be exploited as a direct proof of the ability of the motor to work.

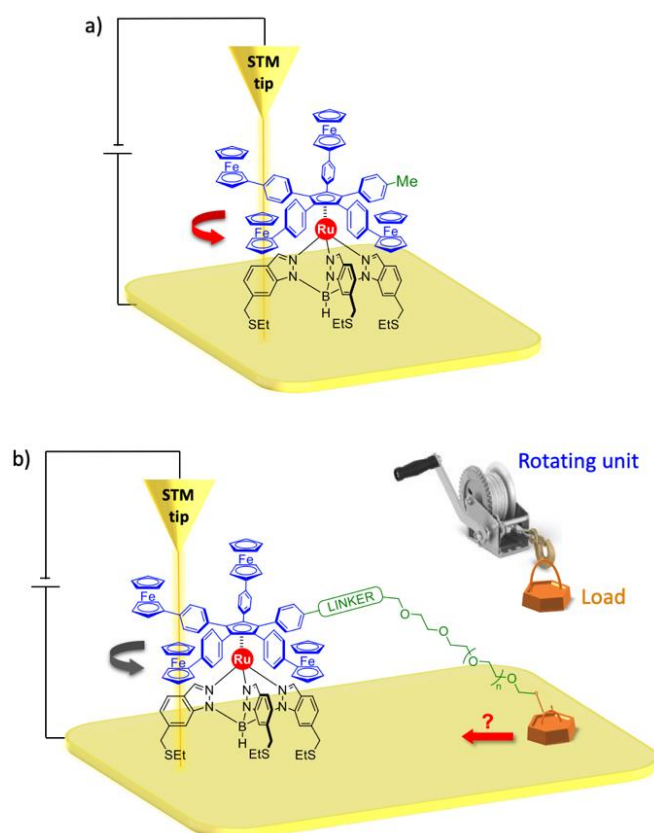


Figure 1. a) Stepwise and unidirectional rotation of the ruthenium-based molecular motor adsorbed on a gold surface at low temperature (5 K) when fueled with electrons delivered by the STM tip; b) Experimental setup envisioned to probe the ability of the motor to provide work: the ruthenium-based motor is embedded in a molecular winch structure, allowing to pull a molecular load (in orange) on the surface upon unidirectional rotation of the rotor subunit (in blue).

It is important to note that at this scale, the weight of the molecular load is not important because momentum can be neglected with respect to the molecule-surface interactions involved in the physisorption process. Motion of the load upon actuation of the motor subunit will thus occur only if the available work surpasses the diffusion energy of the molecular load on the surface. In anticipation of STM studies at the single-molecule scale, the nanowinch will thus be connected to a series of fragments acting as loads with varying diffusion energies. This will first allow to identify one load that is actually pulled by the rotating winch on the surface, thereby proving the capacity of the motor to perform work. Moreover, this strategy will also provide information on the work limit of the motor by probing nanowinches loaded with fragments bearing increasing diffusion energies, up to the point where no motion of the load is observed upon actuation of the motor subunit. Noteworthy, the diffusion energy of all load fragments will be determined experimentally by lateral manipulation with the STM tip, which will in turn allow an estimation of the work limit value.

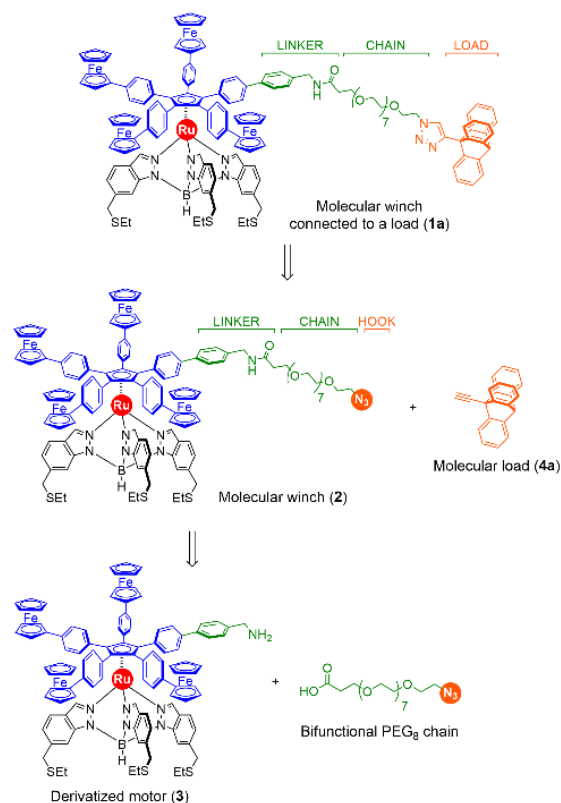
Herein, we report the design and synthesis of a molecular winch, loaded with various molecular fragments such as triptycene, fullerene and porphyrin derivatives. The latter have been selected for their

straightforward imaging capabilities and characteristics by STM, as well as for the previous synthetic knowledge acquired in our group.

RESULTS AND DISCUSSION

1. Design of the molecular winch and of the series of loads

As in macroscopic counterparts, the technomimetic molecular winch envisioned in this work will be composed of three main parts: the rotary motor, a long chain and a terminal hook, allowing the connection of a variety of molecular loads (Scheme 1). Such derivatization of the ruthenium complex should however preserve its function as motor, undergoing directional rotation when fueled with electrons. As prerequisite for our design, the structural and electronic features of the original ruthenium complex thus have to be retained in winch prototypes, which implies a steric and electronic decoupling between the motor subunit and the long chain. The linker should in addition provide thermal stability to the winch prototype in anticipation of on-surface physical vapor deposition.



Scheme 1. Structure of the molecular winch **1a** connected to a triptycyl-9-yl molecular load, and retrosynthetic analysis leading back to the structure of the unloaded molecular winch (**2**) and to the derivatized motor **3** as key intermediate.

Given the broad availability of monodisperse PEG chains functionalized with terminal carboxylic acids, a benzylamide fragment was selected as linker between the chain and the shorter arm of the pentaarylcyclopentadienyl rotor. From a retrosynthetic point of view, the key intermediate in the synthesis of loaded molecular winches such as **1a** would thus be the motor analogue **3**, in which the

truncated tolyl arm is replaced with a pendant 4'-(aminomethyl)biphenyl substituent. A bifunctional PEG₈ chain would be used as coupling partner, with a propionic acid at one extremity and an azide function acting as chemical hook at the other one. A high-yielding copper-catalyzed azide-alkyne cycloaddition could then be exploited to covalently bind a variety of molecular loads to the winch **2** under mild conditions, leading to a 1,2,3-triazole connecting unit in the loaded winch structure.

As mentioned above, a series of alkyne-terminated molecular loads with varying diffusion energies on a gold surface were designed (Figure 2). 9-Ethynyltritycene **4a** was selected as first target since the behavior of the triptycene fragment, in particular its translational motion, has been extensively investigated by STM on various surfaces.^[18] Two molecular loads with higher diffusion energy on gold surface were devised by increasing both the number of triptycene units and the size of the central aromatic backbone. In loads **4c** and **4d**, two (tritypcen-9-yl)ethynyl fragments are thus bound to a benzene ring and to a more extended zinc(II) porphyrin unit, respectively. Finally, [60]-fullerene, a molecular load expected to display a lower diffusion energy than a single triptycene unit was also identified as suitable, easy to visualize,^[19] fragment and fullerene-malonate adduct **4b** was selected as the fourth molecular load.

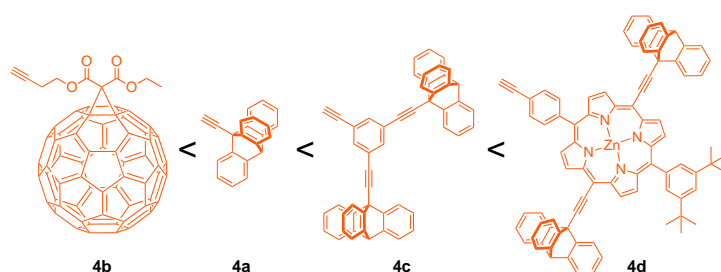
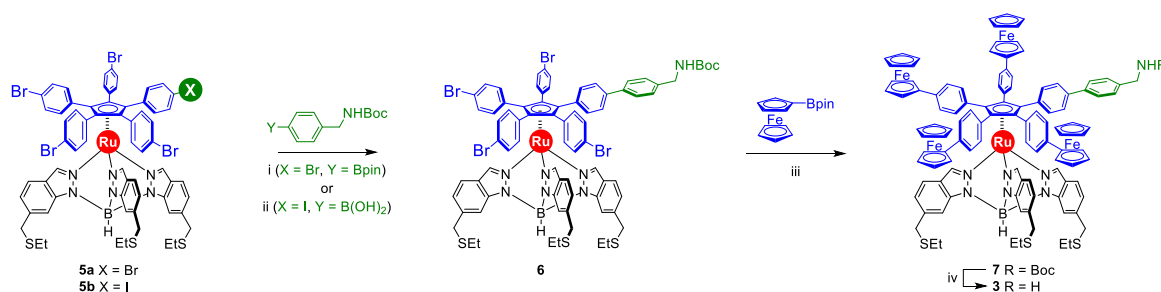


Figure 2. Series of alkyne-terminated molecular loads **4a-4d**, ranked by increasing diffusion energy on surface.

2. Derivatization of the molecular motor

The synthesis of key intermediate **3** was first tackled and a post-functionalization of η^5 -1,2,3,4,5-penta(4-halogenophenyl)cyclopentadienyl ruthenium(II) complex **5** was envisioned, based on our previous work on the synthesis of ruthenium-based molecular machines (Scheme 2).^[9,20] Our strategy involved sequential cross-coupling reactions, with a single bis-aryl coupling in a first step to generate the 4'-(aminomethyl)biphenyl moiety, followed by a four-fold Suzuki-Miyaura reaction to couple the four ferrocene groups.



Scheme 2. Synthesis of the derivatized motor **3**. Reagents and conditions: i) $\text{PdCl}_2(\text{dppf})$ cat., Cs_2CO_3 , $\text{DMF} / \text{H}_2\text{O}$ (1%), 100 °C, 48h, 26%; ii) $\text{Pd}(\text{PPh}_3)_4$ cat., CuTC , THF , 45 °C, 39h, 23%; iii) $\text{PdCl}_2(\text{dppf})$ cat., Cs_2CO_3 , $\text{DMF} / \text{H}_2\text{O}$ (1%), 100 °C, 72h, 42%; iv) TMSOTf , 2,6-lutidine, CH_2Cl_2 , 0°C to RT, 2h, 94%.

This synthetic route was first implemented starting from ruthenium complex **5a**, which incorporates five identical 4-bromophenyl substituents on the cyclopentadienyl ligand. A Suzuki-Miyaura coupling was attempted under statistical conditions using 4-(aminomethyl)phenylboronic acid pinacol ester as coupling partner, the latter being protected as *tert*-butylcarbamate to avoid any side effect of the primary amine during the cross-coupling. A detailed optimization of the reaction conditions was conducted to maximize the yield of monofunctionalized product **6**, among polyfunctionalized side products. Using one equivalent of coupling partner with PdCl₂(dppf) (10 mol%) as catalyst and Cs₂CO₃ (2 equiv.) as base in a DMF / H₂O (1%) mixture at 100 °C, the desired product **6** resulting from a single coupling was obtained in 26% yield.

As opposed to this statistical approach for the monofunctionalization of precursor **5a**, we have recently demonstrated that desymmetrized ruthenium complex **5b**, incorporating a preactivated 4-iodophenyl fragment, undergoes chemoselectively single cross-coupling reactions.^[9b,20] This approach proved particularly efficient for the construction of a single phenylethynyl moiety via Sonogashira coupling, allowing for high levels of iodophenyl vs bromophenyl discrimination in complex **5b**. Bis-aryl couplings appeared more challenging, with no significant selectivity observed under standard Suzuki-Miyaura conditions, such as those mentioned above. However, a combination of Pd(PPh₃)₄ as palladium catalyst with copper(I) thiophene-2-carboxylate (CuTC) as stoichiometric additive, as reported by Savarin and Liebeskind,^[21] allowed for very mild coupling conditions leading selectively to a single biphenyl pattern. Such conditions were thus tested in an attempt to increase the efficiency of the monofunctionalization step, using complex **5b** as precursor and *tert*-butoxycarbonyl (Boc)-protected 4-(aminomethyl)phenylboronic acid as coupling partner. After 24h at 45 °C in THF, the desired product **6** resulting from a single aryl-aryl coupling was obtained in 23% yield. The limited chemoselectivity of this coupling, as compared with previous attempts on precursor **5b** under identical conditions seems to be related to the nature of the coupling partner, with a putative detrimental coordination of the Boc-protected amine to the copper additive. Noteworthy, as Stille reactions have been far more documented for aryl iodide vs aryl bromide discrimination, such a bis-aryl coupling was also attempted on precursor **5b** using the appropriate stannane partner, but it failed to deliver the desired monocoupled product **6** with higher efficiency.

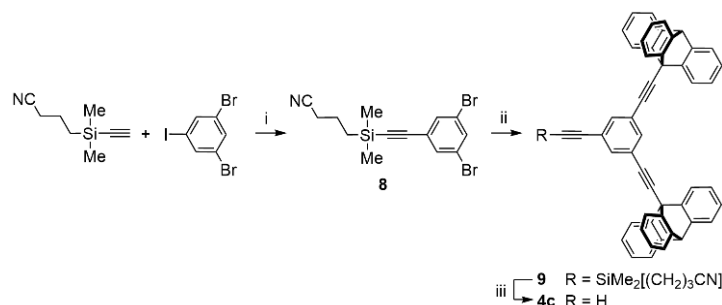
In the next step, the monofunctionalized complex **6**, incorporating four remaining 4-bromophenyl substituents, was submitted to a Suzuki-Miyaura cross-coupling in the presence of a large excess of ferroceneboronic acid pinacol ester. The desired product **7**, resulting from four sequential bis-aryl couplings, was obtained in 42% yield, i.e. 80% per newly-formed C-C bond. Finally, cleavage of the Boc protecting group was achieved under mild conditions, involving trimethylsilyl triflate and 2,6-lutidine in dichloromethane followed by a treatment with methanol, to give the corresponding free benzylamine **3** in 94% yield.

3. Synthesis of the load fragments

Having the key intermediate **3** in our hands, the synthesis of the series of molecular loads bearing a terminal alkyne was tackled. 9-Ethynyltritycene **4a** was prepared according to a standard synthetic route exploited for the synthesis of other molecular machines.^[5] The C₆₀-appended malonate derivative **4b** was obtained in two steps from ethylmalonate as recently reported,^[22] with a Steglich esterification in the presence of but-3-yn-1-ol followed by a Bingel reaction.

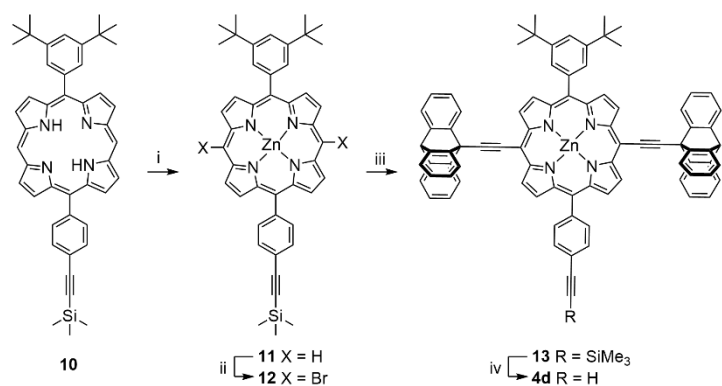
New synthetic routes were devised for the two other molecular loads, incorporating two triptycen-9-ylethynyl moieties around a central benzene (**4c**) or porphyrin (**4d**) core.

3,5-Bis(triptycen-9-ylethynyl)-1-ethynylbenzene (**4c**) was prepared in three steps from 1,3-dibromo-5-iodobenzene, using the (3-cyanopropyl)dimethylsilyl protecting group, a polar analogue of trimethylsilyl,^[23] to facilitate chromatographic purifications along the cross-coupling sequence (Scheme 3). The selective functionalization of the iodinated position with (3-cyanopropyl)dimethylsilylacetylene under mild Sonogashira conditions was followed by a two-fold coupling under harsher conditions with 9-ethynyltriptycene (**4a**) as partner to yield bis-triptycenylic derivative **9**. Final treatment with tetrabutylammonium fluoride (TBAF) allowed the cleavage of the silyl protecting group to give the alkyne-terminated molecular load **4c** in 17% yield over three steps.



Scheme 3. Synthesis of molecular load **4c**. Reagents and conditions: i) $\text{PdCl}_2(\text{PPh}_3)_2$ cat., CuI cat., THF / triethylamine 4:1, RT, 24h, 39%; ii) 9-ethynyltriptycene (**4a**), $\text{PdCl}_2(\text{PPh}_3)_2$ cat., CuI cat., THF / triethylamine 4:1, reflux, 48h, 59%; iii) TBAF, THF , 0 °C to RT, 1h, 72%.

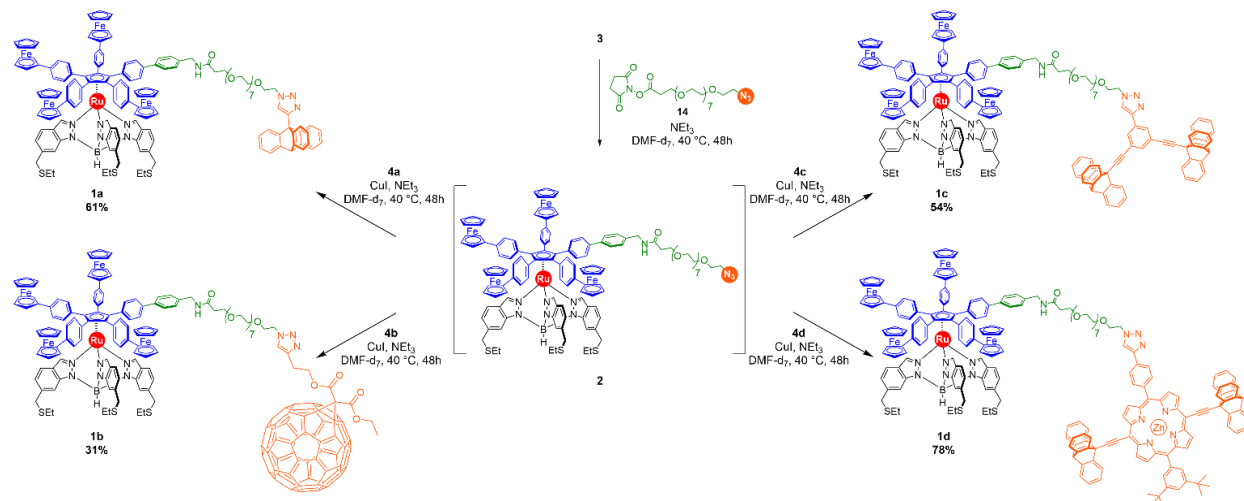
The fourth molecular load (**4d**) incorporates two triptycen-9-ylethynyl fragments connected in a *trans* relationship to a central zinc(II) porphyrin scaffold, with the remaining 5,15 meso positions carrying 4-ethynylphenyl and 3,5-di-*tert*-butylphenyl substituents, respectively. The overall structure of this *trans* A₂BC porphyrin is reminiscent of a series of nanocars reported recently,^[8k] and a similar synthetic route was thus followed (Scheme 4). Free base porphyrin **10**^[24] was prepared from dipyrromethane and the appropriate 3,5-di-*tert*-butyl- and 4-(trimethylsilylethynyl) benzaldehydes under Lindsey conditions and was subsequently metallated in the presence of zinc(II) diacetate. Treatment of zinc(II) porphyrin **11** with *N*-bromosuccinimide resulted in a selective bromination of the 10,20 meso positions, which were then coupled with 9-ethynyltriptycene under Sonogashira conditions to yield the tetrasubstituted A₂BC porphyrin **13**. Finally, cleavage of the trimethylsilyl protecting group using TBAF afforded the target molecular load **4d**, in 45% yield over four steps (from the known free base porphyrin **10**).



Scheme 4. Synthesis of molecular load **4d**. Reagents and conditions: i) $\text{Zn}(\text{OAc})_2 \cdot 2\text{H}_2\text{O}$, CHCl_3 / MeOH 1:1, 45 °C, 16h, 77%; ii) NBS, CH_2Cl_2 / pyridine 40:1, 0 °C to RT, 16h, 78%; iii) 9-ethynyltriptycene (**4a**), $\text{PdCl}_2(\text{PPh}_3)_2$ cat., CuI cat., THF / triethylamine 4:1, reflux, 16h, 91%; iv) TBAF, THF , RT, 1h, 82%.

4. Divergent synthesis of loaded molecular winches

With the four molecular loads and the derivatized motor **3** carrying a pendant benzylamine moiety, the assembly of the molecular winch was addressed. According to the strategy depicted on Scheme 1, a bifunctional PEG₈ chain was required to allow for the formation of both the triazole and benzylamide linkers. The monodisperse precursor **14**, incorporating an azide moiety and a carboxylic acid preactivated as its *N*-hydroxysuccinimidyl ester, was selected and used for all molecular winches in a divergent approach (Scheme 5).



Scheme 5. Divergent synthesis from key precursor **3** of a series of molecular winches carrying a triptycyl (**1a**), bis-triptycyl (**1c** and **1d**) and fullerene (**1b**) fragment as molecular load.

Given the complexity of the target compounds, it was envisioned to perform the sequential condensation and Cu-catalyzed azide-alkyne cycloaddition steps in a single pot by successive addition of reagents and catalysts. The conditions for the click reaction were thus adapted and both steps were finally performed using an excess of triethylamine as base in DMF. To conveniently monitor the progress of each step by ¹H NMR spectroscopy, these small-scale reactions were set up in an NMR tube and deuterated DMF was thus used as solvent.

The benzylamine-appended motor **3** was first reacted with a slight excess of the N₃-PEG₈-NHS chain (**14**, 1.5 equiv.) to afford the desired intermediate **2** with a benzylamide linker after 48h at 40 °C, as observed by ¹H NMR. Addition of 9-ethynyltriptycene (**4a**) and copper(I) iodide to the reaction medium subsequently triggered the azide-alkyne cycloaddition to afford the triazole moiety connecting the PEG chain and the triptycene fragment. The first prototype of molecular winch loaded with a single triptycene (**1a**) was finally isolated in 61% yield over two steps. Full characterization by NMR spectroscopy and high-resolution mass spectrometry unambiguously confirmed the presence of the newly formed benzylamide and triazole moieties, and the 1:1:1 ratio between the motor subunit, the PEG₈ chain and the triptycene load.

The synthesis of the three other loaded molecular winches was achieved according to the same divergent route and exploited ruthenium complex **2** carrying the azide-terminated PEG chain as a common intermediate. Click reaction between azide **2** and alkyne derivatives **4b**, **4c** and **4d** led to a series of molecular winches connected to a variety of loads, such as a C₆₀ fullerene adduct (**1b**, 31% yield) or bis-triptycyl fragments with a central benzene (**1c**, 54% yield) or porphyrin (**1d**, 78% yield) scaffold. In all cases, the conversion for each step was virtually total, as monitored in situ by ¹H NMR, and

differences in isolated yields are related to purification issues. This sequence thus appears particularly efficient for the functionalization of primary amines, e.g. in bioconjugation studies, with a peptide coupling and a Cu-catalyzed azide-alkyne cycloaddition performed in a single pot (instead of two synthetic operations^[25]).

CONCLUSION

A molecular winch was designed according to technomimetic principles in order to explore the mechanical properties of an electron-fueled molecular motor and in particular to probe its ability to work, i.e. to pull a load on a surface. The structure of the ruthenium-based motor was thus derivatized and embedded in a winch structure, with a long flexible PEG chain terminated by an azide hook, to allow for the covalent binding of molecular loads via click reactions. To gain information on the work limit of the motor and estimate experimentally its value, load fragments covering a broad range of diffusion energies on gold were selected, based on triptycene, fullerene and porphyrin moieties.

Derivatization of the molecular motor was successfully achieved by sequential cross-coupling reactions involving first the monofunctionalization of a η^5 -1,2,3,4,5-penta(4-halogenophenyl) cyclopentadienyl ruthenium(II) complex. A divergent approach was then implemented to synthesize a family of four loaded nanowinches, with the connection of the PEG chain and of the load fragment performed in a single pot. This sequence involving a peptide coupling followed by a Cu-catalyzed azide-alkyne cycloaddition appears highly valuable for bioconjugation studies.

The four prototypes of loaded molecular winches **1a-1d**, featuring triptycene-, fullerene- and porphyrin-derived loads will be studied by our STM-specialized collaborators at the single molecule scale on metallic surface as soon as possible to investigate the mechanical properties of the motor. It must be noted this concept is adaptable to measure such motive power for other on-surface electron-fueled motors.

EXPERIMENTAL SECTION

Compounds **5a**,^[26] **5b**,^[20] **4a**,^[5] **4b**,^[22] **10**^[24] and [(3-cyanopropyl) dimethylsilyl]acetylene^[23] were synthesized according to previously reported procedures. Compounds **3**, **4c**, **4d**, **6**, **7**, **8**, **9**, **11**, **12** and **13** are described in the Supporting Information All reactions were carried out using standard Schlenk techniques under an argon atmosphere.

Complex 1a

In a J-Young NMR tube was placed complex **3** (7.2 mg, 3.6 μmol , 1.0 eq.) in 500 μL of deuterated *N,N*-dimethylformamide. Then, N_3 -PEG₈-NHS ester (3.2 mg, 5.5 μmol , 1.5 eq.) and triethylamine (2 μL , 14.4 μmol , 4.0 eq.) were added and the resulting solution was degassed by three successive freeze-pump-thaw cycles. The tube was sealed and the solution was heated at 40 °C for 48 hours. The completion of the condensation reaction was monitored by ¹H NMR. Then, under an inert atmosphere (in a glovebox), the tube was opened and copper(I) iodide (0.8 mg, 4.2 μmol , 1.15 eq.) and 9-ethynyltriptycene **4a** (3.0 mg, 10 μmol , 3.0 eq.) were added. The tube was sealed again and heated at 40 °C for a further 48 hours after which the solvents were evaporated. The crude product was dissolved in a minimal amount of dichloromethane, precipitated in methanol, filtered and washed with 10 mL of cold methanol. The resulting solid was once again dissolved in a minimal amount of dichloromethane and precipitated in heptane. The dichloromethane was removed by rotary evaporation, the suspension

filtered and washed with 10 mL of cold pentane. If impurities were observed by NMR, the operation was repeated as many times as necessary to give complex **1a** as an orange amorphous solid in a 61% yield (6.0 mg, 2.2 μmol). $R_f = 0.48$ (SiO_2 , $\text{MeOH}/\text{CH}_2\text{Cl}_2$ 5:95). ^1H NMR (500 MHz, DMF-d_7 , 25 $^\circ\text{C}$): $\delta = 8.70$ (s, 1H, H_g), 8.47 (br. s, 3H, H_6), 8.23 (t, $^3J = 6.0$ Hz, 1H, NH), 8.20 (s, 3H, H_1), 7.63 – 7.53 (m, 10H, H_{13} , H_b , H_b' and H_f), 7.51 (d, $^3J = 8.8$ Hz, 2H, H_{14}), 7.49 – 7.43 (m, 11H, H_3 , $\text{H}_{18,18'}$), 7.35 (AA'BB' pattern, $^3J = 8.7$ Hz, 8H, $\text{H}_{19,19'}$), 7.30 (AA'BB' pattern, $^3J = 8.5$ Hz, 2H, H_q), 7.12 – 6.97 (m, 9H, H_4 , H_a and H_a'), 5.78 (s, 1H, H_d), 4.94 (t, $^3J = 5.3$ Hz, 2H, H_h), 4.73 (m, 8H, $\text{H}_{22,22'}$), 4.37 (d, $^3J = 6.0$ Hz, 2H, H_o), 4.29 (m, 8H, $\text{H}_{23,23'}$), 4.16 – 4.06 (m, 8H, H_8 and H_i), 3.95 (s, 10H, H_{24} or $\text{H}_{24'}$), 3.94 (s, 10H, H_{24} or $\text{H}_{24'}$), 3.74 – 3.67 (m, 4H, H_j and H_j or H_k), 3.63 – 3.57 (m, 2H, H_j or H_k), 3.54 – 3.49 (m, 24H, H_j and H_k), 2.64 (q, $^3J = 7.4$ Hz, 6H, H_9), 2.46 (t, $^3J = 6.3$ Hz, 2H, H_m), 1.34 (t, $^3J = 7.4$ Hz, 9H, H_{10}) ppm. $^{13}\text{C}\{^1\text{H}\}$ NMR (126 MHz, DMF-d_7 , 25 $^\circ\text{C}$): $\delta = 170.7$ (C^n), 146.7 (C^c or $\text{C}^{c'}$), 146.6 (C^c or $\text{C}^{c'}$), 144.1 (C^2), 143.3 (C^f), 140.4 (C^1), 139.7 (C^s), 139.4 (C^p), 139.0 (C^{20} and $\text{C}^{20'}$), 138.5 (C^{15}), 137.3 (C^5), 134.4 (C^{13}), 133.9 (C^{18} or $\text{C}^{18'}$), 133.8 (C^{18} or $\text{C}^{18'}$), 132.0 (C^{17} or $\text{C}^{17'}$), 131.9 (C^{17} or $\text{C}^{17'}$), 128.2 (C^q), 127.7 (C^g), 126.7 (C^r), 125.7 (C^a or $\text{C}^{a'}$), 125.0 (C^a or $\text{C}^{a'}$), 124.9 (C^{14} , C^{19} and $\text{C}^{19'}$), 124.2 (C^b or $\text{C}^{b'}$), 123.9 (C^b or $\text{C}^{b'}$), 123.2 (C^4), 122.5 (C^7), 120.1 (C^3), 112.4 (C^6), 88.9 (C^{11}), 88.2 (C^{16} or $\text{C}^{16'}$), 86.9 (C^{16} or $\text{C}^{16'}$), 84.2 (C^{21} and $\text{C}^{21'}$), 70.6 (C^i , C^j and/or C^k), 70.5 (C^i , C^j and/or C^k), 70.3 (C^i , C^j and/or C^k), 70.0 (C^{24} and $\text{C}^{24'}$), 69.6 (C^i , C^j and/or C^k), 69.5 (C^{23} and $\text{C}^{23'}$), 67.5 (C^l), 66.6 (C^{22} and $\text{C}^{22'}$), 55.2 (C^e), 54.2 (C^d), 50.4 (C^h), 42.4 (C^o), 37.6 (C^8), 36.9 (C^m), 27.4 (C^9), 14.3 (C^{10}) ppm. Quaternary carbon C^{12} could not be unambiguously assigned using 2D NMR experiments. HR-MS (MALDI): calcd. for $\text{C}_{153}\text{H}_{147}\text{BFe}_4\text{N}_{10}\text{O}_9\text{RuS}_3$ [M] $^+$: 2701.7119, found 2701.7070.

Complex 1b

In a J-Young NMR tube was placed complex **3** (7.8 mg, 3.9 μmol , 1.0 eq.) in 500 μL of deuterated *N,N*-dimethylformamide. Then, N_3 -PEG₈-NHS ester (3.3 mg, 5.9 μmol , 1.5 eq.) and triethylamine (2.2 μL , 16.0 μmol , 4.0 eq.) were added and the resulting solution was degassed by three successive freeze-pump-thaw cycles. The tube was sealed and the solution was heated at 40 $^\circ\text{C}$ for 48 hours. The completion of the condensation reaction was monitored by ^1H NMR. Then, under an inert atmosphere (in a glovebox), the tube was opened and copper(I) iodide (0.6 mg, 3.2 μmol , 0.8 eq.) and the C_{60} fullerene adduct **4b** (7.1 mg, 7.9 μmol , 2.0 eq.) were added. The tube was sealed again and heated at 40 $^\circ\text{C}$ for a further 48 hours after which the solvents were evaporated. The crude product was dissolved in a minimal amount of dichloromethane and precipitated in methanol, filtered and washed with 10 mL of cold methanol. The resulting solid was once again dissolved in a minimal amount of dichloromethane and precipitated in heptane. The dichloromethane was removed by rotary evaporation, the suspension filtered and washed with 10 mL of cold pentane. Pure product was recovered in dichloromethane and the solvent was evaporated to dryness to give complex **1b** as an orange amorphous solid in a 31% yield (4.0 mg, 1.2 μmol). R_f value could not be determined for this compound due to relatively low solubility in most organic solvents inducing important tailing on TLC. ^1H NMR (500 MHz, DMF-d_7 , 25 $^\circ\text{C}$): 8.97 (br. s, 1H, H_i), 8.29 (m, 1H, NH), 8.26-8.16 (m, 6H, H_6 and H_1), 7.72 – 7.03 (m, 30H, H_3 , H_4 , H_{13} , H_{14} , $\text{H}_{18,18'}$, $\text{H}_{19,19'}$, H_8 and H_t), 4.91 – 4.87 (m, 2H, H_j), 4.73 (br. s, 8H, $\text{H}_{22,22'}$), 4.62 – 4.54 (m, 4H, H_b and H_f), 4.37 (d, $^3J = 6.1$ Hz, 2H, H_q), 4.30 (br. s, 8H, $\text{H}_{23,23'}$), 4.04 – 3.87 (m, 28H, H_g , H_8 , $\text{H}_{24,24'}$), 3.48 (m, 34H, H_k , H_l , H_m , H_n and H_o), 2.56 – 2.43 (m, 6H, H_9), 1.46 – 1.40 (m, 3H, H_a), 1.32 – 1.21 (m, 9H, H_{10}) ppm. $^{13}\text{C}\{^1\text{H}\}$ NMR (126 MHz, DMF-d_7 , 25 $^\circ\text{C}$): $\delta = 170.7$ (C^c , C^e or C^p), 170.4 (C^c , C^e or C^p), 167.9 (C^c , C^e or C^p), 145.4 (C^{quat}), 145.3 (C^{quat}), 145.3 (C^{quat}), 144.8 (C^{quat}), 144.7 (C^{quat}), 144.0 (C^{quat}), 143.1 (C^{quat}), 142.1 (C^{quat}), 141.0 (C^{quat}), 139.6 (C^{quat}), 139.1 (C^{quat}), 138.9 (C^{quat}), 134.5 (C^{13}), 133.9 (C^{18} and $\text{C}^{18'}$), 131.8 (C^{17} and $\text{C}^{17'}$), 129.3 ($\text{C}_{\text{Ar-H}}$), 128.6 ($\text{C}_{\text{Ar-H}}$), 128.2 ($\text{C}_{\text{Ar-H}}$), 126.8 ($\text{C}_{\text{Ar-H}}$), 125.6 ($\text{C}_{\text{Ar-H}}$), 124.9 ($\text{C}_{\text{Ar-H}}$), 123.5 (C^4), 122.4 (C^7), 120.3 (C^3), 116.5 (C^i), 111.8 (C^6), 84.2 (C^{Cp}), 78.0 (C^{Cp}), 70.6 ($\text{OCH}_2\text{CH}_2\text{O}$), 70.5 ($\text{OCH}_2\text{CH}_2\text{O}$), 70.4 ($\text{OCH}_2\text{CH}_2\text{O}$), 70.1 (C^{24} and $\text{C}^{24'}$), 69.6 (C^{23} and $\text{C}^{23'}$), 67.6 (CH_2), 66.7 (C^{22} and $\text{C}^{22'}$), 65.9 (CH_2), 64.1 (C^b or C^f), 50.2 (C^b or C^f), 42.4 (C^q), 36.9 (CH_2), 36.1 (C^8),

32.1 (CH₂), 25.9 (CH₂), 25.8 (C⁹), 14.5 (C^a), 14.1 (C¹⁰) ppm. Due to the very low solubility of compound **1b** inducing a poor resolution of NMR spectra, part of the signals could not be unambiguously assigned and are labelled C^{quat}, C^{Cp}, C_{Ar}-H, OCH₂CH₂O or CH₂. HR-MS (MALDI): calcd. for C₂₀₀H₁₄₃BFe₄N₁₀O₁₃RuS₃ [M]⁺: 3325.6611, found 3325.6589.

Complex 1c

In a J-Young NMR tube was placed complex **3** (6.6 mg, 3.3 μmol, 1.0 eq.) in 500 μL of deuterated *N,N*-dimethylformamide. Then, N₃-PEG₈-NHS ester (2.3 mg, 4.0 μmol, 1.2 eq.) and triethylamine (3 μL, 22 μmol, 6.5 eq.) were added and the resulting solution was degassed by three successive freeze-pump-thaw cycles. The tube was sealed and the solution was heated at 40 °C for 48 hours. The completion of the condensation reaction was monitored by ¹H NMR. Then, under an inert atmosphere (in a glovebox), the tube was opened and copper(I) iodide (0.8 mg, 4.2 μmol, 1.3 eq.) and alkyne **4c** (3.7 mg, 5.7 μmol, 1.7 eq.) were added. The tube was sealed again and heated at 40 °C for a further 48 hours, after which the solvents were evaporated. The crude product was dissolved in a minimal amount of dichloromethane and precipitated in methanol, filtered, and washed with 10 mL of cold methanol. The resulting solid was once again dissolved in a minimal amount of dichloromethane and precipitated in heptane. The dichloromethane was removed by rotary evaporation, the suspension filtered and washed with 10 mL of cold pentane. Pure product was recovered in dichloromethane and the solvent was evaporated to dryness to give complex **1c** as an orange amorphous solid in a 54% yield (5.6 mg, 1.8 μmol). *R*_f = 0.23 (SiO₂, MeOH/CH₂Cl₂ 20:80). ¹H NMR (500 MHz, DMF-d₇, 25 °C): δ = 8.98 (s, 1H, H_m), 8.74 – 8.68 (m, 3H, H_j and H_h), 8.61 (br. s, 3H, H₆), 8.21 (br. s, 4H, H₁ and NH), 7.97 (dd, ³*J* = 7.3 Hz, ⁴*J* = 1.4 Hz, 6H, H_b'), 7.62 – 7.54 (m, 10H, H_b, H_x and H₁₃), 7.53 – 7.43 (m, 13H, H₃, H₁₄, H_{18,18'}), 7.38 – 7.32 (m, 8H, H_{19,19'}), 7.29 (AA'BB' pattern, ³*J* = 8.2 Hz, 2H, H_w), 7.21 – 7.12 (m, 12H, H_a and H_{a'}), 7.11 – 7.07 (m, 3H, H₄), 5.86 (s, 2H, H_d), 4.77 – 4.71 (m, 8H, H_{22,22'}), 4.40 – 4.35 (m, 2H, H_u), 4.31 – 4.27 (m, 8H, H_{23,23'}), 4.23 (br. s, 6H, H₈), 4.02 (t, ³*J* = 5.1 Hz, 2H, H_r), 3.96 – 3.94 (m, 20H, H_{24,24'}), 3.73 – 3.46 (m, 32H, H_n, H_o, H_p and H_q), 2.80 – 2.76 (m, 6H, H₉), 2.48 – 2.43 (m, 2H, H_s), 1.39 (t, ³*J* = 7.3 Hz, 9H, H₁₀) ppm. ¹³C{¹H} NMR (126 MHz, DMF-d₇, 25 °C): δ = 170.7 (Cⁱ), 145.5 (C^l), 145.3 (C^c), 144.8 (C^c), 144.1 (C²), 140.4 (C¹), 139.7 (C^{quat-Ar}), 139.4 (C^{quat-Ar}), 139.1 (C²⁰, C^{20'}), 138.5 (C^{quat-Ar}), 136.6 (C⁵), 135.2 (C^h), 134.4 (C¹³), 133.9 (C¹⁸ or C^{18'}), 133.8 (C¹⁸ or C^{18'}), 133.2 (C^{quat-Ar}), 132.0 (C¹⁷ or C^{17'}), 131.9 (C¹⁷ or C^{17'}), 129.7 (C^j), 128.2 (C^w), 126.8 (C^x), 126.4 (C^a), 125.7 (C^{a'}), 125.0 (C¹⁴, C¹⁹ or C^{19'}), 124.9 (C¹⁹ or C^{19'}), 124.3 (C^{quat-Ar}), 124.2 (C^b), 123.6 (C^m), 123.3 (C⁴), 122.7 (C^{b'}), 122.6 (C⁷), 120.2 (C³), 113.0 (C⁶), 92.3 (C^g), 88.9 (C¹¹), 88.2 (C¹⁶ or C^{16'}), 86.9 (C¹⁶ or C^{16'}), 85.2 (C^f), 84.2 (C²¹ and C^{21'}), 70.6 (OCH₂CH₂O), 70.3 (OCH₂CH₂O), 70.1 (C²⁴ and C^{24'}), 69.5 (C²³ and C^{23'}), 67.5 (C^r), 66.6 (C²² and C^{22'}), 53.9 (C^e), 52.8 (C^d), 50.7 (OCH₂CH₂O), 42.4 (C^u), 38.9 (C⁸), 36.9 (C^s), 28.9 (C⁹), 14.2 (C¹⁰) ppm. C^{quat-Ar} = Cⁱ, C^k, C^v, C^y, C¹², C¹⁵ for which signals could not be unambiguously assigned using HMBC NMR; one of these signals corresponds to two non-equivalent carbons with identical chemical shifts. HR-MS (MALDI): calcd. for C₁₈₃H₁₆₃BFe₄N₁₀O₉RuS₃ [M]⁺: 3077.8374, found 3077.8424.

Complex 1d

In a J-Young NMR tube, complex **3** (7.5 mg, 3.8 μmol, 1.0 eq.) was dissolved in 500 μL of deuterated *N,N*-dimethylformamide. Then, N₃-PEG₈-NHS ester (1.9 mg, 3.4 μmol, 0.9 eq.) and triethylamine (3 μL, 22 μmol, 5.7 eq.) were added and the resulting solution was degassed by three successive freeze-pump-thaw cycles. The tube was sealed and the solution was heated at 40 °C for 48 hours. Then, under an inert atmosphere (in a glovebox), the tube was opened and copper(I) iodide (0.14 mg, 0.76 μmol, 20 mol%) and porphyrin **4d** (4.6 mg, 3.8 μmol, 1.0 eq.) were added. The tube was sealed again and heated at 40 °C for a further 48 hours. After confirming the complete conversion of the alkyne to a triazole by ¹H NMR, the solvents were evaporated. The crude product was purified by column chromatography (SiO₂, MeOH/CH₂Cl₂ 2.5:97.5 to 10:90) to give complex **1d** as a dark green amorphous solid in a 78% yield (10.8 mg, 3.0 μmol). *R*_f = 0.34 (SiO₂, MeOH/CH₂Cl₂ 8:92). ¹H NMR (500 MHz,

DMF-d₇, 25 °C): δ = 10.14 (m, 4H, H _{β}), 9.14 (d, 3J = 4.5 Hz, 2H, H _{β}), 9.08 (d, 3J = 4.5 Hz, 2H, H _{β}), 8.93 (s, 1H, H _{γ}), 8.51 – 8.43 (m, 9H, H _{i} and H _{i}), 8.26 – 8.12 (m, 9H, H _{e} , H _{6} , H _{u} and H _{v}), 8.01 (m, 3J = 1.9 Hz, 1H, H _{d}), 7.73 (d, 3J = 7.2 Hz, 6H, H _{i}), 7.62 – 7.56 (m, 2H, H _{13}), 7.54 – 7.40 (m, 13H, H _{3} , H _{14} and H _{$18,18'$}), 7.38 – 7.20 (m, 24H, H _{j} , H _{k} , H _{$19,19'$} , H _{26} and H _{27}), 7.07 (d, 3J = 8.4 Hz, 3H, H _{4}), 6.03 (s, 2H, H _{n}), 4.81 (t, 3J = 7.4 Hz, 2H, H _{36}), 4.69 (m, 8H, H _{$22,22'$}), 4.33 – 4.28 (m, 2H, H _{29}), 4.26 (m, 8H, H _{$23,23'$}), 4.11 – 4.05 (m, 2H, H _{35}), 3.99 – 3.87 (m, 26H, H _{8} and H _{$24,24'$}), 3.48 (m, 30H, H _{32} , H _{33} and H _{34}), 2.54 – 2.44 (m, 6H, H _{9}), 2.39 (t, 3J = 6.4 Hz, 2H, H _{31}), 1.61 (s, 18H, H _{a}), 1.29 (d, 3J = 7.3 Hz, 9H, H _{10}) ppm. $^{13}\text{C}\{^1\text{H}\}$ NMR (126 MHz, DMF-d₇, 25 °C): δ = 170.6 (C³⁰), 152.6 (C ^{α}), 152.5 (C ^{α}), 151.0 (C ^{α}), 150.7 (C ^{α}), 149.3 (C ^{ϵ}), 147.0 (C ^{x}), 145.6 (C ^{h} and C ^{m}), 144.1 (C^{quat-Ar} and C^{quat-Ar}), 142.2 (C ^{f} or C ^{l}), 142.0 (C ^{f} or C ^{l}), 139.6 (C^{quat-Ar}), 139.4 (C^{quat-Ar}), 139.1 (C^{quat-Ar}), 139.0 (C⁵ or C²⁰ and C^{20'}), 138.7 (C^{quat-Ar}), 138.5 (C⁵ or C²⁰ and C^{20'}), 135.4 (C¹), 134.4 (C¹³), 133.8 (C ^{β}), 133.7 (C¹⁸ and C^{18'}), 133.6 (C ^{β}), 131.9 (C¹², C¹⁷ and C^{17'}), 131.4 (C ^{β}), 131.3 (C ^{β}), 130.1 (C ^{e}), 128.2 (C²⁷ and C¹⁴), 126.7 (C²⁶), 126.5 (C ^{k}), 126.0 (C ^{j}), 124.9 (C¹⁹, C^{19'}), 124.8 (C ^{u} or C ^{v}), 124.6 (C ^{g}), 124.5 (C¹), 124.1 (C ^{u} or C ^{v}), 122.9 (C ^{i} and C⁴), 122.6 (C ^{y}), 122.4 (C ^{s}), 121.8 (C ^{d}), 120.2 (C³), 111.5 (C⁶), 100.3 (C ^{p} or C ^{q} or C ^{r}), 96.0 (C ^{p} or C ^{q} or C ^{r}), 91.1 (C ^{p} or C ^{q} or C ^{r}), 88.8 (C¹¹), 88.2 (C¹⁶ or C^{16'}), 86.9 (C¹⁶ or C^{16'}), 84.2 (C²¹ and C^{21'}), 70.7 (C³³, C³⁴ and/or C³⁵), 70.6 (C³³, C³⁴ and/or C³⁵), 70.5 (C³³, C³⁴ and/or C³⁵), 70.4 (C³³, C³⁴ and/or C³⁵), 70.3 (C³³, C³⁴ and/or C³⁵), 70.1 (C²⁴ and C^{24'}), 69.6 (C³³, C³⁴ and/or C³⁵), 69.5 (C²³ and C^{23'}), 67.5 (C³²), 66.6 (C²² and C^{22'}), 55.2 (C ^{o}), 53.0 (C ^{n}), 50.5 (C³⁶), 42.3 (C²⁹), 36.8 (C³¹), 36.1 (C⁸), 35.2 (C ^{b}), 31.6 (C ^{a}), 25.3 (C⁹), 14.5 (C¹⁰) ppm. C ^{b} and C¹¹ did not appear on the $^{13}\text{C}\{^1\text{H}\}$ NMR spectrum but its chemical shift was assigned thanks to correlation on HMBC NMR spectrum; C^{quat-Ar} = C ^{w} , C², C⁷, C¹⁵, C²⁵ and C²⁸ for which signals could not be unambiguously assigned using HMBC NMR. UV-Vis (CH₂Cl₂): λ_{max} (ϵ) = 246 (sh, 13 900), 416 (sh, 60 100), 439 (435 500), 449 (sh, 270 000), 581 (14 000), 620 (20 000), 685 nm (51 100 mol⁻¹dm³cm⁻¹). HR-MS (MALDI): calcd. for C₂₁₇H₁₉₃BFe₄N₁₄O₉RuS₃Zn [M]⁺: 3638.0134, found 3638.0133.

ACKNOWLEDGEMENTS

This work was supported by the University Paul Sabatier (Toulouse) and CNRS. It has received funding from the European Union's Horizon 2020 research and innovation programme under the project MEMO, grant agreement No 766864, the JSPS KAKENHI Grant-in-Aid for Challenging Research (20K21131). Y. G. thanks the French Ministry of National Education for a PhD Fellowship. Technical assistance provided by the services of the Institut de Chimie de Toulouse ICT-UAR 2599 is gratefully acknowledged, and the authors thank Dr. Nathalie Saffon-Merceron for her valuable help regarding crystallographic analysis. Dr. Julien Monot and Dr. Andrej Jancarik are warmly acknowledged for fruitful discussions.

REFERENCES

- [1] V. Balzani, A. Credi, M. Venturi, in *Molecular Devices and Machines – A Journey into the Nano World*, Wiley-VCH Weinheim, **2003**.
- [2] a) J.-P. Sauvage, *Angew. Chem. Int. Ed.* **2017**, *56*, 11080–11093; *Angew. Chem.* **2017**, *129*, 11228–11242; b) J. F. Stoddart, *Angew. Chem. Int. Ed.* **2017**, *56*, 11094–11125; *Angew. Chem.* **2017**, *129*, 11244–11277; c) B. L. Feringa, *Angew. Chem. Int. Ed.* **2017**, *56*, 11060–11078; *Angew. Chem.* **2017**, *129*, 11206–11226.
- [3] G. Rapenne, *Org. Biomol. Chem.* **2005**, *3*, 1165–1169; b) A. A. Gakh, *Molecular Devices: An Introduction to Technomimetics and Its Biological Applications*, John Wiley & Sons, Hoboken, NJ, **2018**; c) C. Kammerer, G. Erbland, Y. Gisbert, T. Nishino, K. Yasuhara, G. Rapenne, *Chem. Lett.* **2019**, *48*, 299–308.
- [4] T. Muraoka, K. Kinbara, Y. Kobayashi, T. Aida, *J. Am. Chem. Soc.* **2003**, *125*, 5612–5613.
- [5] G. Rapenne, G. Jimenez-Bueno, *Tetrahedron* **2007**, *63*, 7018–7026.
- [6] A. Ikeda, T. Tsudera, S. Shinkai, *J. Org. Chem.* **1997**, *62*, 3568–3574.

- [7] J. D. Badjić, V. Balzani, A. Credi, S. Silvi, J. F. Stoddart, *Science* **2004**, *303*, 1845–1849.
- [8] a) G. Vives, J. M. Tour, *Acc. Chem. Res.* **2009**, *42*, 473–487; b) H.-P. Jacquot de Rouville, R. Garbage, R. E. Cook, A. R. Pujol, A. M. Sirven, G. Rapenne, *Chem. Eur. J.* **2012**, *18*, 3023–3031; c) H.-P. Jacquot de Rouville, R. Garbage, F. Ample, A. Nickel, J. Meyer, F. Moresco, C. Joachim, G. Rapenne, *Chem. Eur. J.* **2012**, *18*, 8925–8928; d) W.-H. Soe, Y. Shirai, C. Durand, Y. Yonamine, K. Minami, X. Bouju, M. Kolmer, K. Ariga, C. Joachim, W. Nakanishi, *ACS Nano* **2017**, *11*, 10357–10365; e) G. Rapenne, C. Joachim, *Nat. Rev. Mater.* **2017**, *2*, 1–3; f) F. Eisenhut, C. Durand, F. Moresco, J.-P. Launay, C. Joachim, *Eur. Phys. J. Appl. Phys.* **2016**, *76*, 10001.; g) W.-H. Soe, C. Durand, S. Gauthier, H.-P. Jacquot de Rouville, C. Kammerer, G. Rapenne, C. Joachim, *Nanotechnology* **2018**, *29*, 495401; h) T. Kudernac, N. Ruangsupapichat, M. Parschau, B. Maci, N. Katsonis, S. R. Harutyunyan, K. H. Ernst, B. L. Feringa, *Nature* **2011**, *479*, 208–211; i) R. Pawlak, T. Meier, N. Renaud, M. Kisiel, A. Hinaut, T. Glatzel, D. Sordes, C. Durand, W.-H. Soe, A. Baratoff, C. Joachim, C. E. Housecroft, E. C. Constable, E. Meyer, *ACS Nano* **2017**, *11*, 9930–9940; j) G. J. Simpson, V. García-López, P. Petermeier, L. Grill, J. M. Tour, *Nat. Nanotechnol.* **2017**, *12*, 604–606; k) T. Nishino, C. J. Martin, H. Takeuchi, F. Lim, K. Yasuhara, Y. Gisbert, S. Abid, N. Saffon-Merceron, C. Kammerer, G. Rapenne, *Chem. Eur. J.* **2020**, *26*, 12010–12018.
- [9] a) G. Erbland, S. Abid, Y. Gisbert, N. Saffon - Merceron, Y. Hashimoto, L. Andreoni, T. Guérin, C. Kammerer, G. Rapenne, *Chem. Eur. J.* **2019**, *25*, 16328–16339; b) S. Abid, Y. Gisbert, M. Kojima, N. Saffon-Merceron, J. Cuny, C. Kammerer, G. Rapenne, *Chem. Sci.* **2021**, *12*, 4709–4721.
- [10] S. Kassem, A. T. L. Lee, D. A. Leigh, A. Markevicius, J. Solà, *Nat. Chem.* **2016**, *8*, 138–143.
- [11] a) T. R. Kelly, H. D. Silva, R. A. Silva, *Nature* **1999**, *401*, 150–152; b) N. Koumura, R. W. J. Zijlstra, R. A. van Delden, N. Harada, B. L. Feringa, *Nature* **1999**, *401*, 152–155; c) D. A. Leigh, J. K. Y. Wong, F. Dehez, F. Zerbetto, *Nature* **2003**, *424*, 174–179; d) H. L. Tierney, C. J. Murphy, A. D. Jewell, A. E. Baber, E. V. Iski, H. Y. Khodaverdian, A. F. McGuire, N. Klebanov, E. C. H. Sykes, *Nat. Nanotechnol.* **2011**, *6*, 625–629; e) U. G. E. Perera, F. Ample, H. Kersell, Y. Zhang, G. Vives, J. Echeverria, M. Grisolia, G. Rapenne, C. Joachim, S.-W. Hla, *Nat. Nanotechnol.* **2013**, *8*, 46–51; f) Y. Zhang, J. P. Calupitan, T. Rojas, R. Tumbleson, G. Erbland, C. Kammerer, T. M. Ajayi, S. Wang, L. A. Curtiss, A. T. Ngo, S. E. Ulloa, G. Rapenne, S.-W. Hla, *Nat. Commun.* **2019**, *10*, 3742; g) G. J. Simpson, V. García-López, A. Daniel Boese, J. M. Tour, L. Grill, *Nat. Commun.* **2019**, *10*, 4631; h) S. Kassem, T. van Leeuwen, A. S. Lubbe, M. R. Wilson, B. L. Feringa, D. A. Leigh, *Chem. Soc. Rev.* **2017**, *46*, 2592–2621; i) V. García-López, D. Liu, J. M. Tour, *Chem. Rev.* **2020**, *120*, 79–124; j) A. Goswami, S. Saha, P. K. Biswas, M. Schmittel, *Chem. Rev.* **2020**, *120*, 125–199; k) M. Baroncini, S. Silvi, A. Credi, *Chem. Rev.* **2020**, *120*, 200–268; l) D. Dattler, G. Fuks, J. Heiser, E. Moulin, A. Perrot, X. Yao, N. Giuseppone, *Chem. Rev.* **2020**, *120*, 310–433.
- [12] R. A. van Delden, M. K. J. ter Wiel, M. M. Pollard, J. Vicario, N. Koumura, B. L. Feringa, *Nature* **2005**, *437*, 1337–1340.
- [13] R. Eelkema, M. M. Pollard, J. Vicario, N. Katsonis, B. S. Ramon, C. W. M. Bastiaansen, D. J. Broer, B. L. Feringa, *Nature* **2006**, *440*, 163–163.
- [14] J. T. Foy, Q. Li, A. Goujon, J.-R. Colard-Itté, G. Fuks, E. Moulin, O. Schiffmann, D. Dattler, D. P. Funeriu, N. Giuseppone, *Nat. Nanotechnol.* **2017**, *12*, 540–545.
- [15] a) For an example of molecular motor in the 1-5 nm size range studied by Single Molecule Force Spectroscopy, see: P. Lussis, T. Svaldo-Lanero, A. Bertocco, C.-A. Fustin, D. A. Leigh, A.-S. Duwez, *Nat. Nanotechnol.* **2011**, *6*, 553–557; b) For an example of biomolecular motor in the 80-200 nm size range studied using magnetic tweezers, see: X. Hu, X. Zhao, I. Y. Loh, J. Yan, Z. Wang, *Nanoscale* **2021**, *13*, 13195–13207; c) J. H. Marden, L. R. Allen, *Proc. Natl. Acad. Sci. USA* **2002**, *99*, 4161–4166.
- [16] G. Vives, G. Rapenne, *Tetrahedron* **2008**, *64*, 11462–11468.
- [17] C. Kammerer, G. Rapenne, *Eur. J. Inorg. Chem.* **2016**, 2214–2226.
- [18] a) Y. Makoudi, E. Duverger, M. Arab, F. Chérioux, F. Ample, G. Rapenne, X. Bouju, F. Palmino, *Chem. Phys. Chem.* **2008**, *9*, 1437–1441; b) X. Bouju, F. Chérioux, S. Coget, G. Rapenne, F. Palmino, *Nanoscale* **2013**, *5*, 7005–7010; c) W.-H. Soe, C. Durand, S. Gauthier, H.-P. Jacquot de Rouville, C. Kammerer, G. Rapenne, C. Joachim, *Nanotechnology* **2018**, *29*, 495401.
- [19] Y. Shirai, A. J. Osgood, Y. Zhao, K. F. Kelly, J. M. Tour, *Nano Lett.* **2005**, *5*, 2330–2334.
- [20] Y. Gisbert, S. Abid, G. Bertrand, N. Saffon-Merceron, C. Kammerer, G. Rapenne, *Chem. Commun.* **2019**, 55, 14689–14692.
- [21] C. Savarin, L. S. Liebeskind, *Org. Lett.* **2001**, *3*, 2149–2152.
- [22] F.-A. Teng, Y. Guo, J. He, Y. Zhang, Z. Han, H. Li, *Des. Monomers Polym.* **2017**, *20*, 283–292.
- [23] S. Höger, K. Bonrad, *J. Org. Chem.* **2000**, *65*, 2243–2245.
- [24] D. Gao, S. M. Aly, P.-L. Karsenti, G. Brisard, P. D. Harvey, *Phys. Chem. Chem. Phys.* **2017**, *19*, 2926–2939.
- [25] Q. Wang, T. R. Chan, R. Hilgraf, V. V. Fokin, K. B. Sharpless, M. G. Finn, *J. Am. Chem. Soc.* **2003**, *125*, 3192–3193 and references cited therein.
- [26] G. Erbland, Y. Gisbert, G. Rapenne, C. Kammerer, *Eur. J. Org. Chem.* **2018**, 4731–4739.